Numerical study of Rayleigh wave transmission through an acoustic barrier

Ebrahim Lamkanfi,[1,a)] Nico F. Declercq,[2,b)] Wim Van Paepegem,[1] and Joris Degrieck[1]
[1]*Department of Materials Science and Engineering, Ghent University, Sint-Pietersnieuwstraat 41, 9000 Ghent, Belgium*
[2]*George W. Woodruff School of Mechanical Engineering, Georgia Institute of Technology, 801 Ferst Drive, Atlanta, Georgia 30332-0405, USA and Georgia Tech Lorraine, UMI Georgia Tech-CNRS 2958, 2 rue Marconi, 57070 Metz, France*

(Received 18 December 2008; accepted 10 April 2009; published online 1 June 2009)

Recent experiments [N. F. Declercq and E. Lamkanfi, Appl. Phys. Lett. **93**, 2 (2008)] showed evidence of the relationship between the generation of leaky Rayleigh waves and the formation of the two reflected lobes and a null strip for bounded beam incidence at the Rayleigh angle. The evidence was based on an experimental setup using a sound barrier on a liquid solid interface. The current paper presents a finite element investigation of the experiments and confirms the earlier conclusions. In addition, unexplained experimental observations are clarified. Furthermore, a detailed investigation of the influence of the bonding properties between the barrier and the solid on the observed radiation patterns is achieved, which is of broader importance to the nondestructive characterization of bonding in general. © *2009 American Institute of Physics*.
[DOI: 10.1063/1.3130405]

I. INTRODUCTION

When a bounded ultrasonic beam is incident from a liquid onto a solid, longitudinally polarized sound is transferred from the liquid into transmitted longitudinal and shear waves in the solid and into reflected longitudinal sound. At a certain angle of incidence beyond the critical angles corresponding to the lateral longitudinal and shear waves in the solid, a leaky Rayleigh wave is generated. This angle is called the Rayleigh angle. At the Rayleigh angle a lateral shift in the reflected beam is usually visible and is called the Schoch effect, typically accompanied by a null strip in the radiation pattern separating a specular lobe and a nonspecular lobe. The Schoch effect[1] and the presence of the null strip[2] are thoroughly studied effects both experimentally[3,4] and theoretically.[5–10] The conclusions from the past can be summarized as follows. At the Rayleigh angle Rayleigh waves are generated. Simultaneously the Schoch effect with or without a null strip occurs. Only recently conclusive experimental evidence was presented that the Schoch effect (with or without the generation of a null strip) is produced by the accompanying leaky Rayleigh waves. The experimental evidence is based on the use of a sound barrier positioned on a solid substrate immersed in water.[11] The experiments also revealed certain phenomena that could not be explained. A thorough theoretical study is necessary and therefore presented in the current paper. First simulations will be reported on the interaction of a bounded beam at the Rayleigh angle using the finite element method (FEM). This is done to verify that the technique works and that the results are in agreement with the experiments. Then, just as in the experiment, a sound barrier will be constructed on a solid plate and the interaction of the bounded beam with the structure will be studied. The conclusions drawn in the experimental paper[11] will be examined, followed by a study of the influence of the different parameters on the observed phenomena with special attention to phenomena that remained unexplained in the experimental paper.

II. OUTLINE OF EXPERIMENTS

The acousto-optic Schlieren image of Fig. 1 is taken from Ref. 11 and depicts the phenomena under examination. Apart from the incoming sound beam on the left hand side, a complicated diffracted sound pattern is visible on the right hand side. Both sides are separated by a specially constructed sound barrier consisting of two thin microscope slides. Their position is clarified by means of two vertical lines in Fig. 1.

The sound barrier, schematically shown in Fig. 2, is constructed as follows. First, a thick horizontal glass plate of 10 cm is used on which leaky Rayleigh waves can exist. Then a glass barrier is constructed by means of two microscope

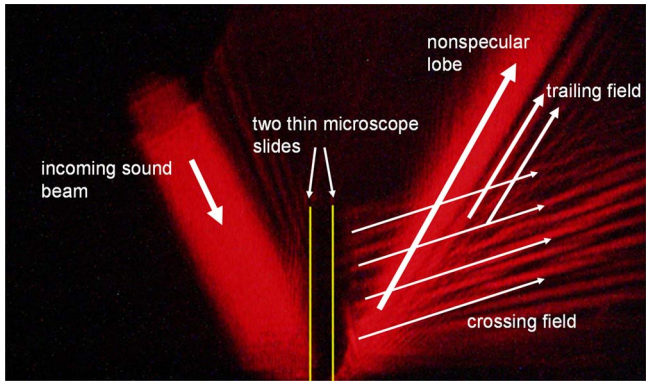

FIG. 1. (Color online) Acousto-optic Schlieren picture of the Schoch effect where the bounded beam coincides with null strip base (Ref. 11).

[a)]Author to whom correspondence should be addressed. Electronic addresses: ebrahim.lamkanfi@ugent.be and elamkanf@gmail.com.
[b)]Electronic mail: nico.declercq@me.gatech.edu.

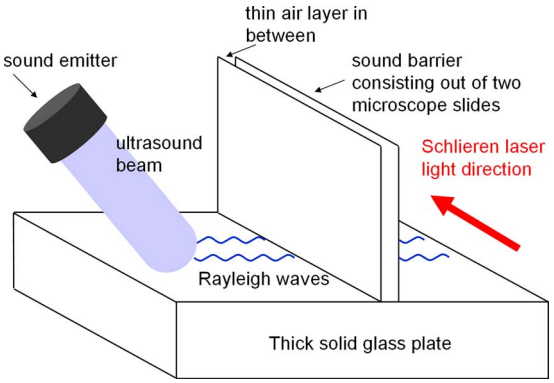

FIG. 2. (Color online) Schematic of experimental setup: sound incident on the left side generates Rayleigh waves that tunnel through the vertical acoustic barrier.

slides placed at a certain distance from each other with a gap in between filled by air. Therefore, because of the impedance mismatch between glass and air, practically no sound energy propagates directly through the barrier. The thickness of the glass plate is 1.6 cm.

When the sound barrier is now moved toward the spot of incidence by numerically changing its position, the sound reaching the opposite side of the barrier must have passed underneath the barrier in the solid. The complexity of the problem requires numerical simulations based on the FEM. In what follows, we apply the FEM to analyze the formation of the second lobe behind the sonic barrier.

III. NUMERICAL PROCEDURE

During the past few decades, the increase in computing power has led to an augmented use of numerical methods in almost every scientific discipline. The FEM, which represents a general class of techniques for the approximate solution of partial differential equations, has proven, among others, its ability to tackle complex scientific and engineering problems successfully. In the finite element formulation of acoustic-structural problems, a coupled acoustic-structural problem, as discussed above, is approximated by dividing the complex geometry into n elements and solving the governing equations in those elements iteratively. These partial differential equations are derived from the conservation law of linear momentum and obtained for the coupled system existing of a solid volume (the glass plate and barriers) in contact with the fluid medium (water) through a boundary surface. The solid is described by the differential equation of motion for a continuum volume assuming small deformations and the fluid by the acoustic wave equation. Additional coupling conditions at their interface have also to be satisfied to ensure the continuity of displacement and pressure between the latter two regions.

As in the real experiment[11] the transducer is first modeled as boundary condition for a harmonic bounded Gaussian ultrasonic beam. The fluid and the solid medium are taken into account with an interaction interface supporting the mechanical continuity equations. Subsequently, the angle of incidence is varied until the Rayleigh angle ϑ^R is obtained. As in experiments, retrieving the Rayleigh angle corresponds to observing the formation of the Schoch effect, usually accompanied by a null strip in between specular and nonspecular lobes, as schematically depicted in Fig. 3.

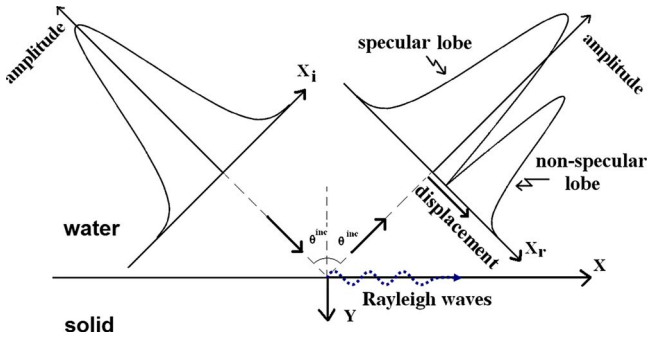

FIG. 3. (Color online) Schematic principle of the Schoch effect.

According to Ref. 11, the nonspecular lobe is a superposition of a directly reflected sound field and a leakage field generated by the generated Rayleigh wave. Leaky Rayleigh waves propagate in the solid, are confined to the interface, and may propagate or "tunnel" underneath a sound barrier placed on the surface. Theoretical verification of the earlier reported experiments[11] is done by proving that the sound field appearing behind the sound barrier is due to tunneled Rayleigh waves and not by other scattered waves.

IV. NUMERICAL RESULTS

A. Schoch effect on a surface without sound barrier

First, as mentioned above, the 3 MHz bounded Gaussian beam is modeled having a beam width of 6 mm, which is comparable to the width of the transducer generating this ultrasound beam in the experimental setup. Moreover, a glass plate, large enough to ignore edge effects, is completely immersed in water for which the following material parameters are taken: a density of $\rho_L = 1000\ \mathrm{kg/m^3}$ and a bulk modulus of $B = 2.25 \times 10^9\ \mathrm{N/m^2}$. The material properties for glass are Young's modulus $E = 7.0 \times 10^{10}\ \mathrm{N/m^2}$, Poisson's ratio $\nu = 1/3$, and density $\rho_S = 2500\ \mathrm{kg/m^3}$. Once this basic configuration is established, the Rayleigh angle is found by changing the angle of incidence in steps of 0.1°. For the mentioned material parameters, the Rayleigh angle is 29°. Figures 4(a)–4(d) show the results for different angles of interest,

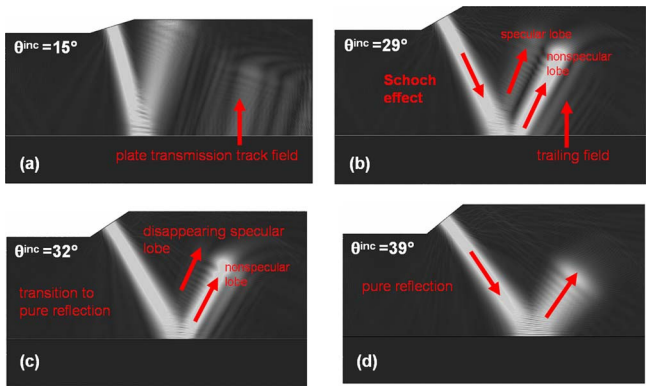

FIG. 4. (Color online) Search for the right critical angle for the formation of the Schoch effect (with null strip).

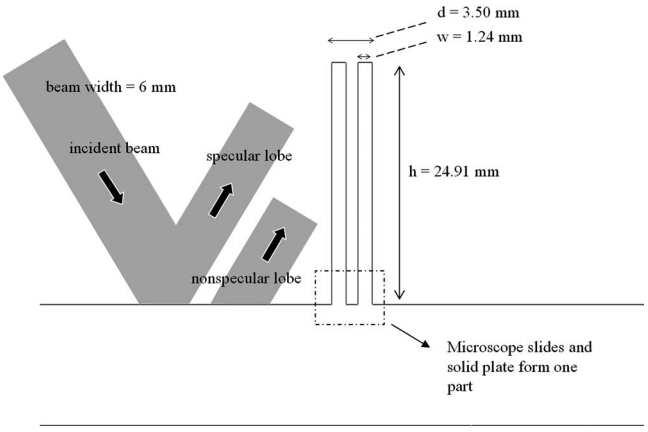

FIG. 5. Dimensions of the sound barrier effect.

including the Rayleigh angle at 29°, as in Ref. 11. The intensity values shown in the numerical simulations are obtained by averaging the square root of the pressure values over one period. Moreover, a bilinear patterning curve is applied on this intensity field making different pressure regions that have an intensity larger than a certain threshold value better visible. This explains why certain wave patterns, which are not visualized with the Schlieren photography method, can still be observed in the numerical simulations.

As seen in Fig. 4(a), angles smaller than the Rayleigh angle result in re-emission of sound behind the reflected beam due to reflection of the transmitted bulk waves on the back surface of the solid, which are in turn transmitted back into the liquid. This results in a clear intensity field behind the first reflected zone of the incident beam. As the incident angle reaches and surpasses the Rayleigh angle, the trailing field disappears almost completely and all the energy is concentrated along the interface, a phenomenon typically connected to evanescent waves beyond the second critical angle of incidence. In what follows, the angle of incidence is fixed at the Rayleigh angle.

B. Implementation of sound barrier with perfect bonding

The basic model discussed in Sec. IV A is now extended with the implementation of the sound barrier. First, the solid plate and the microscope slides are modeled as one "monolithic" block, which, as a first approach, is realistic since all the materials involved constitute the same glass material. The dimensions of the sound barrier are depicted in Fig. 5: the width of the microscope slides that form the barrier is $w=1.24$ mm and the height is $h=24.91$ mm. Apart from the two microscope slides, as in the experiment, a thin layer of air is modeled in between.

Subsequently the sound barrier is moved closer to the spot of incidence of the beam. The numerical results for four different relative positions of the sound barrier and the incident beam are shown in Fig. 6. Whereas the Schoch effect is still visible in Fig. 6(a), it vanishes gradually through Figs. 6(b) and 6(c) as the sound barrier is moving closer to the incident spot of the ultrasonic beam on the solid plate. Finally, when the sound barrier is placed right in the null strip of the reflected beam pattern, still a nonspecular sound field is generated behind the sound barrier [Fig. 6(d)]. Just as in the experiment in Ref. 11, this proves that a nonspecular sound field is formed by reradiation of Rayleigh waves, possibly in combination with directly reflected sound depending on whether the latter is allowed or prohibited by a sound barrier. Therefore, so far, the numerical results are in agreement with what has been described in Ref. 11. Nevertheless there are some discrepancies left that are due to the simplified assumptions concerning the bonding between the sound barrier and the solid. In reality[11] the microscope slides have been glued to the surface and therefore the numerical simulations must be further extended. This will be done in Sec. IV C.

Even in the simplified case described, there are interesting physical phenomena to observe concerning Rayleigh waves that are in agreement with earlier reports[6,12] and that are of interest for the physical behavior of the studied waves upon interaction with barriers. At the left side of the barrier in Fig. 6(d), a diffracted field can be observed which intensifies as the sound barrier approaches the spot of incidence. Moreover, the intensity of the second lobe at the right side of the barrier and the additional field that crosses this second

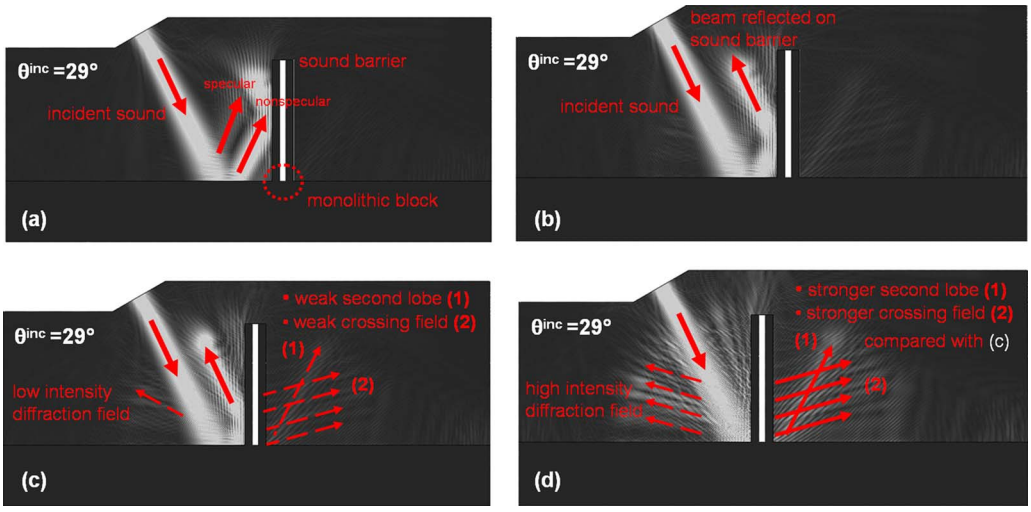

FIG. 6. (Color online) Moving the sound barrier to the spot of generation of the second lobe.

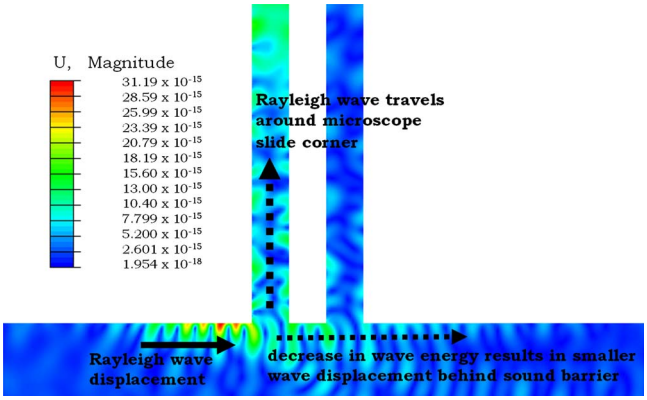

FIG. 7. (Color online) Propagation of Rayleigh waves around the corner of the microscope slides.

lobe increases compared with the case in Fig. 6(c), but still has a significantly lower intensity in comparison with the experiments.[11]

The difference in beam intensity behind the barrier actually means that a smaller portion of the incident energy is transmitted through the barrier. This is explained as follows. Close investigation of the region where the solid-liquid interface is bonded to the microscope slide shows that the generated Rayleigh waves at the left side of the barrier do not bridge the gap completely because they are partially traveling upward along the water-microscope slide interface. This is shown in Fig. 7 where a significant part of the wave displacement can be found in the leftmost microscope slide, resulting in a significant loss of energy transmission of the Rayleigh waves at the right side of the barrier.

A similar phenomenon, but on a different structure, has been reported in an earlier study,[6,12] where it was shown that Rayleigh waves have a specific characteristic of traveling around corners.

C. Implementation of sound barrier incorporating adhesive properties

The presence of an adhesive layer between the microscope slides and the solid will moderate the scattering effect of Rayleigh waves when they encounter the sound barrier. This moderation will determine how much of the Rayleigh wave intensity passes underneath the barrier and how much is sent directly into the microscope slides themselves. The more sound passing underneath the barrier, the more intense the re-emitted sound field after the barrier should be; the more sound sent into the microscope slides, the more a leakage field becomes visible at the left side of the barrier due to the re-emission of sound energy by waves propagating upward the microscope slide [Fig. 8(a)].

The adhesive layer between the microscope slide and the solid is modeled as a thin layer having material properties with the characteristics of a Loctite® bonding material used in the experiments.[11] Because adhesives in general have significantly lower Young's modulus than the solid plate and the microscope slides, generally in the order from 2 to 5 $\times 10^9$ N/m^2, this particular parameter is varied in order to investigate its influence on the transmission efficiency. First,

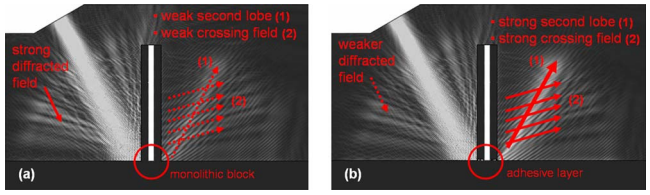

FIG. 8. (Color online) Modeling the interface as a monolithic block (a) or with an adhesive layer has an influence on the intensity of the diffracted field at the left and the second lobe and the crossing field at the right.

a comparison is made between the results in the situation with and without the adhesive layer. A very prominent characteristic, as seen in Fig. 8(b), is that the adhesive layer makes the intensity of the sound field behind the barrier increase drastically.

A more pronounced field behind the barrier does indeed correspond to the experimental observation and is evidence of the importance of the adhesive layer. Still, there is an entire spectrum of adhesive properties possible and their influence on the transmission is a particular point of interest for acoustic barriers in general and for a specific experiment as studied in this paper.

It is found that materials with rather high Young's modulus [$E=200\times 10^9$ N/m^2 in Fig. 9(a)] prevent almost all Rayleigh waves from penetrating the microscope slide, resulting in a strong and clear scattering field in front of the barrier. As a consequence a large decrease in energy transmission is obtained with low intensity values for the leakage field and the crossing field behind the barrier. Moreover, the second lobe has completely disappeared. In the case of low Young's moduli [Fig. 9(b)] the opposite effect occurs. The scattered field on the left hand side of the sound barrier has completely vanished due to an increase in wave energy transmission underneath the sound barrier. This occurs for Young's modulus of 2×10^9 N/m^2, which is a common value for adhesives.

Furthermore it is possible to optimize Young's modulus and to obtain almost a perfect agreement with the experiment,[11] as shown in Fig. 10. Here, the scattered field on the left hand side of the sound barrier disappears completely, whereas the second lobe and the crossing field are still visible with intensity values comparable to those of Fig. 8(b).

V. CONCLUSION

The FEM is employed to study the interaction of a bounded beam with a thick solid plate having a sound barrier

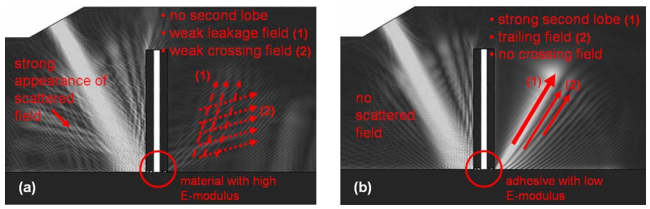

FIG. 9. (Color online) Influence of Young's modulus on the energy transmission through the barrier: high value of (a) $E=200\times 10^9$ N/m^2 and a low one of (b) $E=2\times 10^9$ N/m^2.

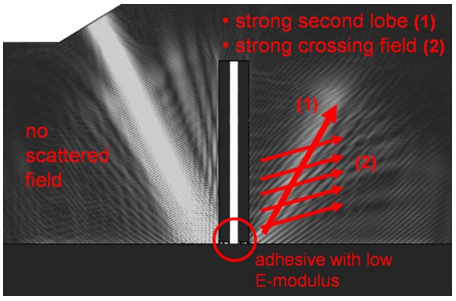

FIG. 10. (Color online) Optimization of the adhesive layer parameters.

at the tip surface. Numerical evidence is presented that the nonspecular lobe in the Schoch effect is, as commonly assumed, due to leaky Rayleigh waves. After a short discussion of the numerical procedure, the validity of the method is shown by reconstructing the Schoch effect on a liquid-solid interface. The implementation of a sound barrier in the finite element model resulted in the formation of a nonspecular sound field behind the barrier. This is only possible due to the propagation of Rayleigh waves underneath the barrier. Moreover, by incorporating an adhesive layer between the barrier and the solid plate, it is shown that Young's modulus of the adhesive has an important effect on the transmission efficiency of Rayleigh waves. Optimization of this material parameter resulted in a good agreement with the experimental results.

ACKNOWLEDGMENTS

The authors gratefully acknowledge the financial support from the Fund for Scientific Research-Flanders (FWO).

[1]H. L. Bertoni and T. Tamir, IEEE Trans. Sonics Ultrason. **SU21**, 85 (1974).
[2]W. G. Neubauer, J. Appl. Phys. **44**, 48 (1973).
[3]A. Schoch, Acustica **2**, 1 (1952).
[4]A. Schoch, Acustica **2**, 18 (1952).
[5]M. A. Breazeale, L. Adler, and L. Flax, J. Acoust. Soc. Am. **56**, 866 (1974).
[6]M. A. Breazeale, L. Adler, and G. W. Scott, J. Appl. Phys. **48**, 530 (1977).
[7]N. F. Declercq, A. Teklu, M. A. Breazeale, R. Briers, O. Leroy, J. Degrieck, and G. N. Shkerdin, J. Appl. Phys. **96**, 5836 (2004).
[8]W. G. Neubauer and L. R. Dragonet, J. Appl. Phys. **45**, 618 (1974).
[9]T. D. K. Ngoc and W. G. Mayer, J. Acoust. Soc. Am. **67**, 1149 (1980).
[10]J. Pott and J. G. Harris, J. Acoust. Soc. Am. **76**, 1829 (1984).
[11]N. F. Declercq and E. Lamkanfi, Appl. Phys. Lett. **93**, 2 (2008).
[12]E. Lamkanfi, N. F. Declercq, W. Van Paepegem, and J. Degrieck, J. Appl. Phys. **101**, 10 (2007).